PRELIMINARY BEAM LOSS STUDY OF TPS DURING BEAM COMMISSIONING

C. H. Huang, Demi Lee, Jenny Chen, Y.S. Cheng, K. H. Hu, C. Y. Wu, C. Y. Liao, K. T. Hsu
NSRRC, Hsinchu 30076, Taiwan

Abstract

Taiwan photon source TPS is a 3rd generation and 3 GeV synchrotron light source in NSRRC. Several types of beam loss monitors (BLMs) such as RadFETs and PIN-diode BLMs are installed in the storage ring to understand the beam loss distribution and mechanism during the injection, decay mode, top-up operation and beam trip. Several RadFETs are also installed around the inserting devices to study the beam loss near the linear scalars. The preliminary beam loss study using RadFETs and PIN-diode BLMs in the storage will be summarized in this report.

INTRODUCTION

Taiwan Photon Source (TPS) is a third-generation light source in NSRRC [1]. The circumference of the storage ring is 518.4 m with 24 double-bend achromat cells. There are 6 long-straight sections and 18 standard-straight sections to accommodate insertion devices. During the initial phase of beam-line commissioning with ten inserting devices for seven beam lines, the beam current can be stored more than 500 mA and the beam loss became significant during the high-current stored beam.

To study the beam loss during the commissioning of this stage, the radiation-sensing field-effect transistor (RadFETs) and Bergoz's PIN-diode beam loss monitors (BLMs) are installed in the storage ring. The RadFET, a discrete p-channel metal-oxide-semiconductor field-effect transistor optimized for ionizing radiation, is used to measure the accumulated dose [2] whereas the PIN-diode BLM detects the charge particles and counted during a particular time interval.

In the TPS, the vertical aperture limit locates at elliptically polarized undulators (EPUs) whereas the horizontal aperture limit is at the septa in the injection area. As the gap of the in-vacuum undulators are small enough, there would be another vertical aperture limit. The Coulomb scattering particle is easy to be detected here. Touschek scattered particles would be detected at the location between the 1st and 2nd bending magnet of each cell where dispersion function is highest following the straight section with high current density. Inelastic or Bremsstrahlung scattering particles would be detected in the in-side wall chamber after a bending magnet [3].

EXPERIMENTAL SETUP AND DATA ACQUISITION SYSTEM

Six RadFETs and six PIN-diode BLMs are installed in the inside-wall chamber of each cell as shown in Fig. 1. Several RadFETs are also installed around the EPU48 and EPU46. The threshold voltage, which is corresponding to the accumulated dose with a pre-recorded calibration curve, is read by a home-made reader which is designed up to sixteen channels [4]. Dosage rate is calculated by the EPICS record processing in the EPICS IOC and published into control network. Data acquisition for BLMs is performed by a 16-channel scaler installed on the cPCI carrier board which locates at the cPCI EPICS IOC on the equipment area. All scalers are synchronized by the timing system of the accelerator with 1 second gating time which is programmable with 1 msec step [5].

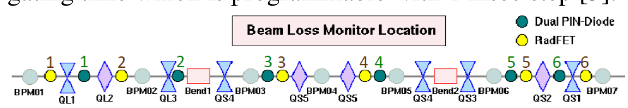

Figure 1: The installation position of six RadFETs and PIN-diode BLMs in each cell. The RadFETs and PIN-diode BLMs in each cell are labelled as position 1 to 6.

The dose rate of RadFETs and counting rate of PIN-diode BLMs are shown in the control system, as in Fig. 2. The threshold voltage of the RadFETs and counting rate of PIN-diode BLMs are stored in the archive system for the further analysis.

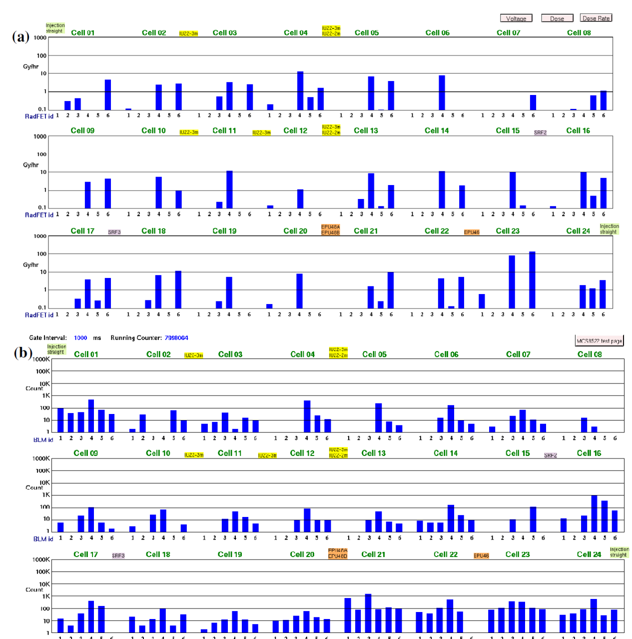

Figure 2: The (a) dose rate distribution of RadFETs and (b) counting rate of PIN-diode BLMs shown in control console.

BEAM LOSS STUDY USING RADFETS

At the end of initial phase beamline commission in December 25th, the threshold voltage, which is corresponding to the accumulated dose, is higher at position #4 and #6 (around 5 m after the bending magnets) in each cell, shown in Fig. 3. It may be because the dispersion is higher around this region in which it is easy to detect the inelastic scattered particles.

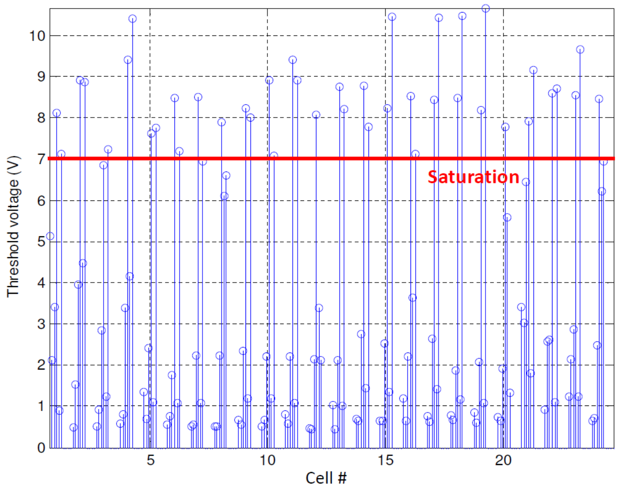

Figure 3: The threshold voltage of RadFETs in December 25th, 2015.

In the low current decay mode, around 25 mA, the average dose rate of each RadFET is all below 0.1 Gy/hr, however, in decay mode for the high current, i.e. 200 mA, the dose rate is much higher especially in the position #4 and #6, shown in Fig. 4.

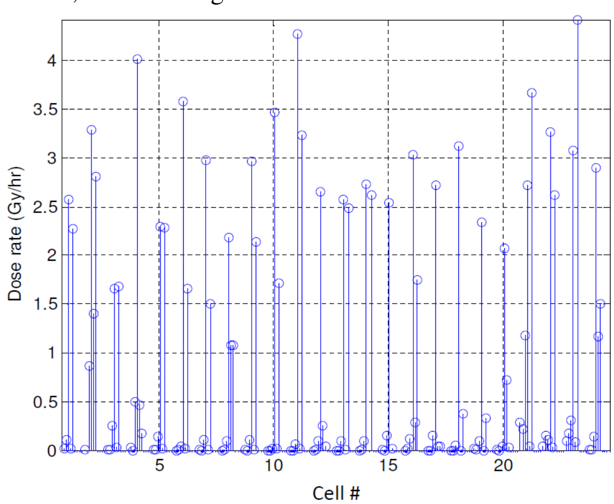

Figure 4: Beam loss pattern during decay mode at beam current around 200 mA.

During the ID commissioning, the linear scalars which are used to measure the gap and phase of EPUs sometimes have a soft error and need to be reset due to the radiation damage. In order to reduce the radiation, a lead shield with 5 mm thickness is put before the EPU48A and EPU48B. At the same time, 2 RadFETs are installed before and behind the lead shield of each EPU48 with one in the upper branch and the other in the lower branch. From the accumulated dose shown in Fig. 5, the radiation in the EPU48B is larger than EPU48A because it is a vertical aperture limit in the double mini-betay (DMBy) between two EPUs and the β_y is relative high around the three quadrupoles between two EPU48s. Therefore the electromagnetic shower produced in the DMBy area would be detected by the RadFETs before the lead shield in the EPU48B. After the lead shield, around half of the radiation could be detected by the RadFETs behind the lead shield.

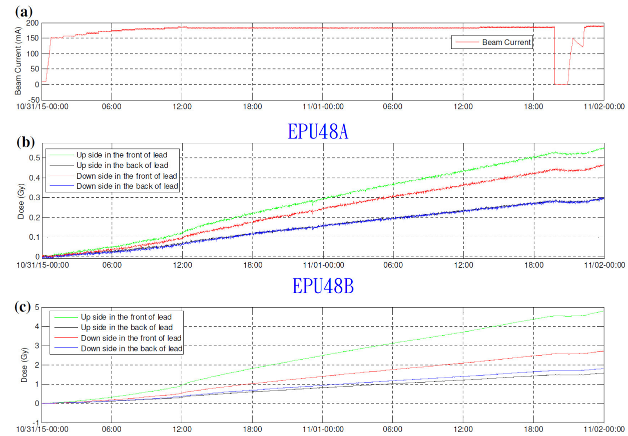

Figure 5: The beam current (a) and the accumulated dose of RadFET installed around the lead shield before (b) EPU48A and (c) EPU48B.

BEAM LOSS STUDY USING PIN-DIODE BEAM LOSS MOINTORS

For the decay mode around 30 mA, the counting rate of PIN-diode BLMs are all below 100 counts per second. In the decay mode around 220 mA, the counting rate could be more than 2000 and the largest one mostly locates in the position #4 of each cell, shown in Fig. 6. When plotting the counting rate v. s. the beam current (I) of the BLM #4 in the 1st cell for example, shown in Fig. 7, the counting rate is mainly proportional to I^2 for the high current. It is also true at the position where the beam loss only contributes from stored beam.

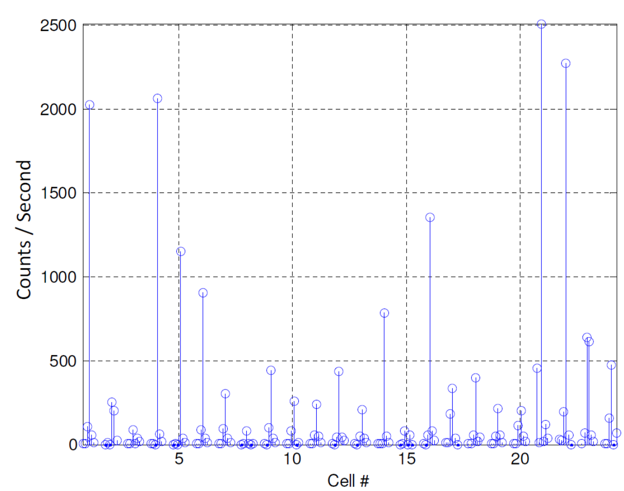

Figure 6: Beam loss distribution during decay mode around 220 mA.

ISBN 978-3-95450-147-2

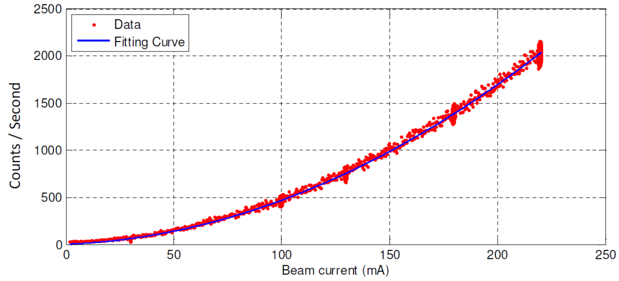

Figure 7: The counting rate of PIN-diode BLM #4 of the 1st cell with various beam current and its fitting curve, counting rate=$0.038I^2+0.87I+4.65$, where I is the beam current.

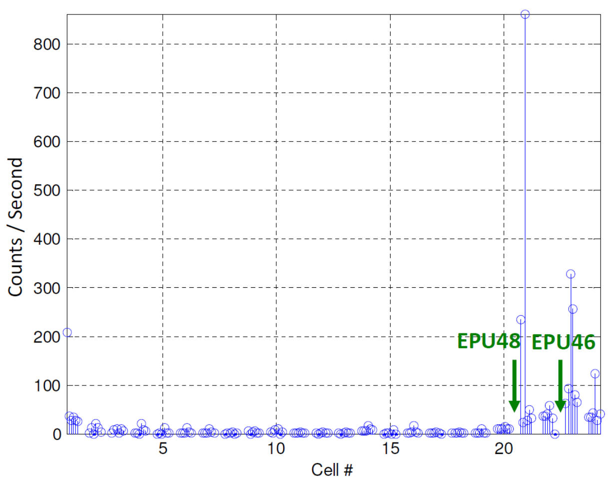

Figure 8: Beam loss distribution during injection from 0 mA to 15 mA.

During the beam injection, the beam loss is mainly detected by BLM #1 at the 1st cell and BLMs at the 21th cell to 24th cell, shown in Fig. 8. The high counting rate at the 21th Cell and the 23th cells are because they locate at downstream of the EPU48 and EPU46 where the vacuum chamber is narrowest in the vertical direction. The high counting rate at BLM #1 of the 1st cell is because it is just following the injection area.

During the beam trip, almost all the BLMs can detect the beam loss, shown in Fig. 9. However, some are still very low or even zero. After preliminary check, these BLMs should be fault or the output pulse are too low to change the status of input signal to the scalar. These BLMs will be replaced to well-functioned ones.

The pattern of beam loss can be divided into 4 categories, as shown in Fig. 10. In the first one, the counting rate of beam loss is mainly contributed by the stored beam such as BLM #4 at the 1st cell. In the second one, the beam-loss count contributes not only from the loss of stored beam but also injection beam such as BLM #4 at 23th cell. In the third category, the counting rate mainly contributes from loss of injection beam such as BLM #1 of the 1st cell. In the last category, the detected counting rate in the injection or high-stored current are both low, but high during the beam trip.

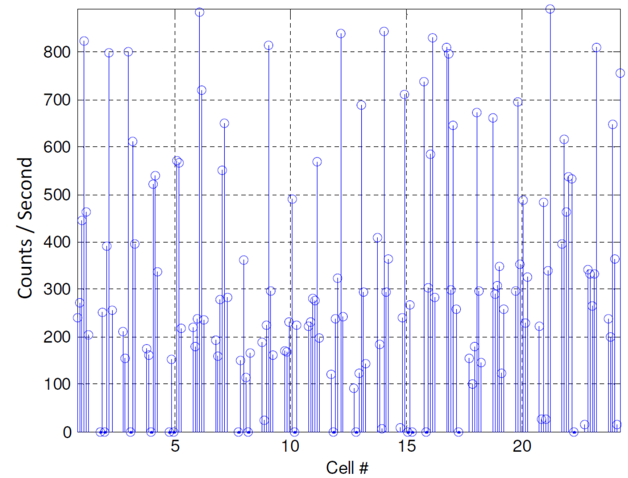

Figure 9: Beam loss distribution during beam trip from 280 mA.

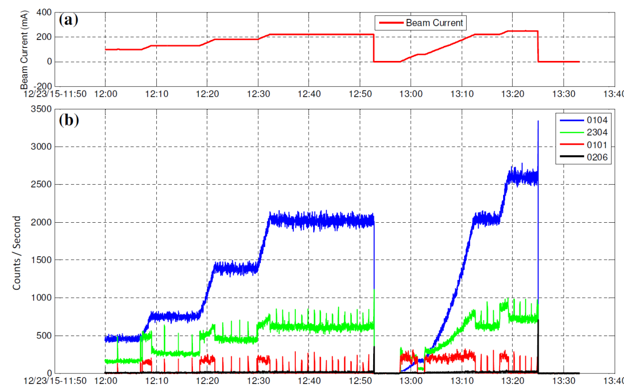

Figure 10: The beam current (a) and (b) beam loss trend of BLMs #4 of the 1st Cell (0104), #4 at the 23th cell (2304), #1 at the 1st cell (0101) and #6 at the 2nd cell (0206).

SUMMARY

RadFETs and PIN-diode BLMs are used to preliminarily study the beam loss during beam commissioning. The RadFETs accumulate high radiation dosage after two bending magnets of each cell during the operation period. Similar pattern can be observed during the decay mode at high current. That is because the inelastic scattering beam will get lost here. For the PIN-diode BLMs, the counting rate are usually high after the first bending magnet where is easy to find the inelastic scattered particles. The loss beam during the injection are observed by the PIN-diode BLMs after the injection area and around the cells which installed the EPUs due to the horizontal and vertical aperture limit. During the beam trip, the beam loss can be detected by almost all BLMs.

REFERENCES

[1] C. C. Kuo, et al., "Commissioning results of the Taiwan Photon Source", in *Proc. IPAC'15*, Richmond, USA, May 2015, paper TUXC3, pp. 1314-1318.

[2] L. Frohich, et al., "Online monitoring of absorbed dose in undulator magnets with RADFET dosimeters at

FERMI@Elettra", Nucl. Instr. And Meth. A, vol. 703, p. 70-79, Mar. 2013.

[3] P. Kuske, "Accelerator physics experiments with beam Loss monitors at BESSY", in *Proc. DIPAC'01*, Grenoble, France, May 2001, paper IT07, pp. 31-35.

[4] D. Lee, et al., "Online RadFET reader for beam loss monitoring system", in Proc. *IPAC'15*, Richmond, USA, May 2015, paper MOPTY070, pp. 1097-1099.

[5] C. H. Huang, et al., "The beam loss monitoring system in Taiwan Photon Source ", in *Proc. IBIC'15*, Melbourne, Australia, Sep. 2015, paper MOPB053, pp. 175-178.

ISBN 978-3-95450-147-2